JOURNAL OF GUIDANCE, CONTROL, AND DYNAMICS
Vol. 25, No. 2, March–April 2002

System Architecture Trades Using Bode-Step Control Design

Boris J. Lurie,* Ali Ghavimi,† Fred Y. Hadaegh,‡ and Edward Mettler*
Jet Propulsion Laboratory, California Institute of Technology, Pasadena, California 91109-8099

The initial stage of a complex system design involves understanding and evaluation of various plant architecture. The conventional approach is to select the configuration of choice via an exhaustive performance evaluation process. The procedure involves designing primitive control laws for each configuration option until the best choice is achieved. This approach is quite time consuming and does not necessarily lead to an optimal choice. An alternative approach is to consider the asymptotic Bode-step technique to arrive at a desired configuration choice. The method is simple and provides a powerful tool in performing system tradeoffs. The method relies on little information regarding plant parameters and does not require any detailed controller design for each system configuration option. The method can easily lend itself to an optimized control strategy that is applicable during both the initial and the final stages of a concept design. The procedure is demonstrated by applying the proposed method to the motion control design of the retroreflector carriage of a spacecraft instrument.

I. Introduction

THE initial stage of a concept design requires understanding of plant properties for multiple system architecture. System dynamics are not well understood, and plant parameters, for example, frequency and damping of structural modes, sensor type and limitations, actuator type and limitations, and sensor and actuator numbers and locations, are not well defined. The selection process for the configuration of choice is usually a tedious task and relies heavily on extensive trade studies provided by both mechanical designers and control engineers.

Underrating the control system performance can lead to a highly complex and overly expensive system design. Therefore, the system configuration of choice can not be finalized before the control systems design is optimized. On the other hand, ignoring issues related to system structural dynamics and the associated plant parameters can also lead to either a costly design or even an unrealizable one. Therefore, the control system design can not be finalized before the architectural and implementation issues are resolved. That is, neither hardware designers nor control engineers can individually dictate a design. In general, appropriate selection of plant parameters is a tedious task and requires extensive interactions between mechanical designers, system engineers, and control engineers to assess the available control performance for multiple system configurations. Such interactions are essential to arrive at a simple and viable system design. This problem is known as control–structure interaction and is shown in Fig. 1.

The control–structure interaction problem may be trivial when a system design is based heavily on a previous design heritage. On the other hand, the control–structure interaction problem can be quite complicated for a new system design. The conventional approach is to find the desired configuration option by means of exhausting iterations because no other practical method yet exists. The strategy is to evaluate the control performance of multiple system architecture by designing preliminary proportional–integral–derivative- (PID-) based control laws for each case. The process generates a system trade matrix through which the configuration options are narrowed.

Received 18 November 1999; revision received 15 September 2000; accepted for publication 22 October 2000.

*Senior Technical Staff, Guidance and Control Analysis Group.
†Senior Technical Staff, Guidance and Control Analysis Group; currently with Masimo Corporation.
‡Senior Research Scientist, Guidance and Control Analysis Group. Associate Fellow AIAA.

The remaining choices are evaluated further by applying more detailed control analysis until the final choice is achieved. Despite the simple nature of the process, the approach is quite time consuming and does not necessarily lead to an optimal design. A different approach is to employ a more sophisticated controller design methodology during the evaluation process; however, the scheme can be quite costly and has little practical feasibility. The main objective of this paper is to propose a simple and powerful tool that is capable of simplifying this tedious design iteration process. The strategy is to evaluate the configuration options via the application of the asymptotic Bode-step method. A system trade matrix is then constructed to facilitate the selection process. Once the final choice is selected, an optimal controller can be designed based on information derived from the associated Bode diagram that was used in the final stage of the selection process.

II. Motivational Examples

The proposed design process is especially well suited for NASA novel space systems. The method is particularly applicable in the framework that NASA engineers perform conceptual designs and simulations and private industries implement detailed design and manufacturing. The following highlights a few examples, where the proposed method proved useful.

Example 1: Cassini Camera Subsystem

In the design process of one of the subsystems of one of the earlier versions of the Cassini spacecraft, it was desired to place a camera at the end of a long flexible boom. Preliminary analyses using PID control laws indicated that the servocontrol system performance is unacceptable in the presence of the system structural modes and a second servosystem was needed to neutralize excess dynamics further. On the other hand, additional analyses using the proposed method revealed that the required control system performance is achievable using only a single servosystem that is substantially simpler, lighter, and cheaper than the implementation proposed by the conventional PID-based approach.

Example 2: Microwave Limb Sounder TeraHertz Antenna Subsystem

The microwave limb sounder TeraHertz antenna beam is required to follow a shallow scanning time profile during an observation cycle, to perform a rapid transition to the dark sky area for calibration at end of each cycle, and to return promptly and settle at rate and position for tracking at the beginning of the next cycle.

Preliminary analyses showed that a single servosystem design based on PID control laws can not reliably meet both the slow scanning accuracy requirements and the fast repositioning requirements. Therefore, a more complicated system was suggested that included two antenna mirrors, the first mirror with its servosystem for slow tracking and the second mirror with its servosystem for fast repositioning. As an alternative approach, the system design using

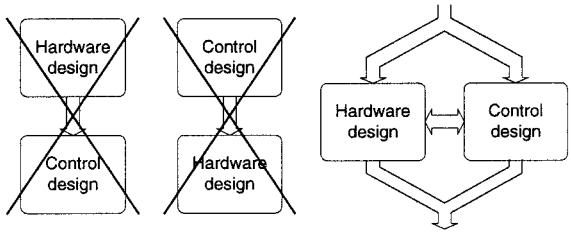

Fig. 1 Control–structure interaction.

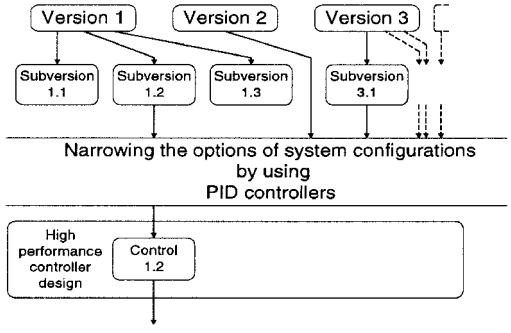

Fig. 2 Conventional system trade of a concept design.

the proposed Bode-step method demonstrated that a single-mirror servomechanism is quite sufficient for both slow tracking and fast repositioning. This led to a viable and cost effective design.

Example 3: Tropospherical Emission Spectrometer Interferometer Subsystem

The interferometer control subsystem of the tropospherical emission spectrometer is required to perform scanning by accurately moving retroreflectors mounted on a carriage assembly. Preliminary analyses using conventional PID methods showed that a single servosystem that consisted of a precision encoder on a motor shaft is not capable of achieving the desired control system performance. It was suggested that an additional laser interferometer sensor was essential in meeting the scanning rate requirements. However, design analyses based on the proposed Bode method illustrated that a single collocated encoder motor is sufficient to meet the performance requirements.

III. System Trades by PID Controllers

Figure 2 is a flow-chart representation of a typical control system design process. The diagram shows that a concept design is studied by examining multiple architectures where each version is also broken up into multiple configuration options. The overall control performance must be evaluated for every individual subversion, whose specifications may require the implementation of multiple servoloops. The conventional approach is to evaluate the available control performance of these configuration options by designing preliminary PID-based control laws for each case.

Once a system trade matrix is obtained, the configuration options are narrowed to a smaller set, and the remaining choices are evaluated further by more detailed control analysis until a final design is achieved. The corresponding control laws are improved further by standard control-related techniques, for example, tuning the system to certain operating conditions, inclusion of possible feedforward methods, or implementation of nonlinear feedback compensation. A better controller design is typically postponed for the final choice of the system configuration because higher performance controller design in the early stage of a design process is commonly believed to be impractical and unjustified, especially, for the case where a design option is not final and may be subject to rejection.

PID-based controller designs are simple; however, they do not provide a systematic procedure for assessing the required control performance, stability, and disturbance rejection. Moreover, the approach requires designing separate controllers for each system configuration option. In addition, the final loop design in each case is not unique, and this makes it difficult to evaluate the resulting trade matrix in a unifying framework. Another important concern is the validity of the results. The difference in disturbance rejection between the PID and a high-performance controller can exceed 10 and even 20 dB (Ref. 1), especially when plants have uncontrollable flexible modes. Therefore, the tradeoff information obtained from a preliminary PID-based design is often erroneous. For example, the system configuration A performs better than B when PID controller methods are employed in both cases, where, in fact, system B is preferable when a high-performance controller design is employed. In this respect, a preliminary PID-based design can lead to hardware design complications, substantial cost impact, or even major system configuration change at a later stage of the design process.

IV. Asymptotic Bode-Step Methods

The Bode-step method is based on Bode integrals that were developed in connection with the conceptual design of wideband feedback amplifiers.[2]

The first Bode integral formula is described by

$$\int_{-\infty}^{\infty} \ell_n |F| \, d\omega = 0$$

where $F = 1 + T$ and T is the negative of the loop transfer function. The feedback at any specific frequency ω is called negative when $|F(j\omega)| > 1$ and positive when $|F(j\omega)| < 1$. The preceding integral formula implies that the area of the negative feedback is equal to the area of positive feedback over the range of all frequencies as shown in Fig. 3.

One of the primary objectives of a control system design is to maximize the area of negative feedback to achieve maximum disturbance rejection over a specified frequency range, typically known as the operational bandwidth. The preceding formula implies that the negative feedback area is maximized if and only if the positive feedback area is maximized. The positive feedback region generally has most of its concentration near the crossover frequency f_b, that is, where $|T(j2\pi f_b)| = 1$. Therefore, a proper loop shaping in the vicinity of f_b is essential for achieving maximum negative feedback over the desired operational frequency bandwidth.

The value of the feedback $|F|$ is given by the distance from the critical point $(-1, 0j)$ to the point on the Nyquist diagram at any given frequency. In light of the preceding integral formula, it then follows that the area of negative feedback is maximized as long as the distance of the Nyquist diagram to the critical point $(-1, 0j)$ is minimized over the frequency range of the positive feedback. This implies that the Nyquist diagram must follow the prescribed stability margin boundaries as close as possible.

Note that the stability margins are defined in terms of possible plant parameter variations and minimum requirements on allowable degrees of process instability.[3,4] The area is typically described by a rectangle on the logarithmic Nyquist plane as shown in Fig. 4

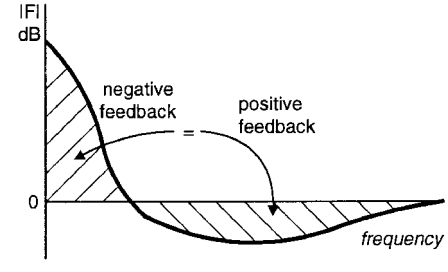

Fig. 3 Feedback as a function of frequency.

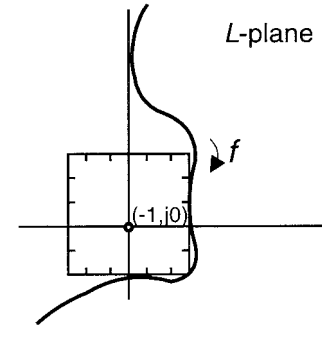

Fig. 4 Stability margin.

because for most plants ignorance of the gain and phase shift is not correlated (Ref. 4, pages 63–64).

The second Bode integral formula is known as Bode phase integral.[2–4] This formula has important design implications and describes tradeoffs between the loop phase lag and the available control performance (disturbance rejection) over the operational bandwidth.

Let (A', φ') and (A'', φ'') represent the gain and phase response pair of two minimum phase transfer functions that have similar high-frequency characteristics. Figure 5 shows the spectrums as a function of frequency. The Bode phase integral is then defined by

$$\Delta A_0 = (A_0'' - A_0') = -\frac{1}{\pi}\int_{-\infty}^{\infty}(\varphi'' - \varphi')\,du$$

where u is the logarithmic frequency, $(A_0'' - A_0')$ is in nepers and $(\varphi'' - \varphi')$ is in radians.

The preceding formula implies that the value of feedback over the operational frequency bandwidth is directly proportional to the value of the associated phase lag. This means that the larger the phase lag, the greater the feedback is in the working band. In other words, the available disturbance rejection is maximized if the loop phase lag is maximized at all frequencies. On the other hand, the global stability considerations limit the amount of phase lag and, consequently, limit the amount of available feedback.

The third Bode integral formula is known as the Bode phase-gain integral[2–4] and in application to the loop responses is described by

$$\phi(\omega_0) = \frac{1}{\pi}\int_{-\infty}^{\infty}\frac{d(\ell_n|T|)}{du}\ell_n\left(\coth\frac{|u|}{2}\right)du$$

where $\phi(\omega_0)$ is the associated minimum phase component of the phase of the loop with gain $\ell_n|T|$ evaluated at the frequency ω_0 and $u = \ell_n(\omega/\omega_0)$. The preceding integral implies that the loop phase at any given frequency is a weighted functional of the loop gain slope at all frequencies. At a closer look, it is seen that $\ell_n(\coth|u|/2)$ scales

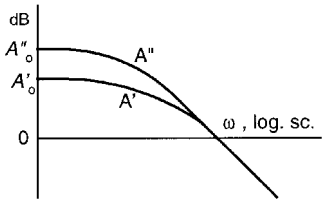

Fig. 5 Spectrum of minimum phase transfer functions.

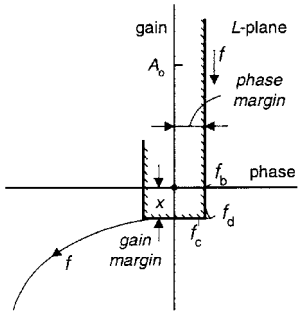

Fig. 6 Bode diagram with Bode step.

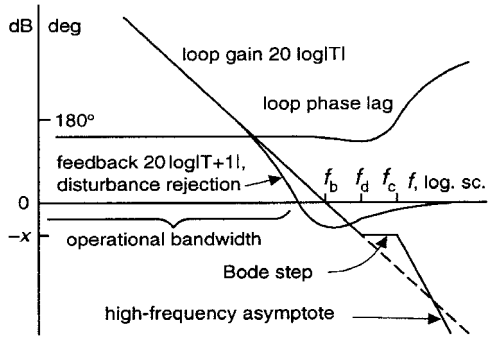

Fig. 7 Asymptotic Bode diagram with Bode step.

the gain slope heavily only at frequencies to within a decade on either side of the frequency point, where the phase is being evaluated.

By further manipulation of the preceding formula, it can be shown that for a loop gain with constant slope of $6n$ dB/octave, the phase can be approximated by $90n$ deg. This gives a useful guideline in shaping the open-loop gain for a specified phase stability margin.

Specifically at higher frequencies, a steep rolloff is usually desired to attenuate the effects of sensor noise and structural modes. However, the third integral formula indicates that such a loop shape at higher frequencies may result in excessive phase lag at the crossover frequency and ultimately leads to instability. This undesired effect can be remedied by designing the loop gain to include a flat piece that extends for 1 or 2 octaves below the 0 dB level by a prescribed gain margin of x dB. This flat segment of the response is known as the Bode step and plays a crucial part in satisfying the high-frequency rolloff requirements and the phase stability margin limitations. Figure 6 shows the Nyquist diagram in the L plane for square stability margins.

Figure 7 shows the Bode diagram representation of the preceding Nyquist diagram. This diagram may be viewed as a transcendental function; however, it can be approximated closely with a high-order rational function for the sake of both detailed design evaluation and controller design implementation.

V. System Trades by Asymptotic Bode-Step Methods

This section describes the application of the Bode integrals for evaluating the performance of multiple system configuration option. The method is applicable to mechanical servosystems and requires only approximate knowledge of structural modes together with the system performance requirements. The method is capable of rapidly predicting information on the available feedback bandwidth, the available disturbance rejection, the required sensor and actuator bandwidth and resolutions, and the required sampling frequency if a digital implementation is desired. Moreover, once the system architecture is finalized, a high-performance controller can easily be realized from the resulting Bode-step design approach. This, in turn, shortens the end-to-end lifecycle of a concept design and provides a simple, viable, and inexpensive solution. The method is by far more advantageous over the conventional approach because it eliminates the number of design iterations. The initial selection process of a conceptual design can be summarized as the following asymptotic Bode step algorithm:

1) Define desired values for phase and gain stability margins, $180y$ deg and x dB, respectively. Typically, $y = \frac{1}{6}$ and $x = 10$ dB (these values necessitate using a prefilter to reduce the overshoot).

2) Approximate the slope of the open-loop gain in the low-frequency range by $-12(1 - y)$ dB per octave.

3) Choose the slope of the loop shape for high-frequency range that is appropriate for rejection of the higher frequencies' effects of sensor noise, plant uncertainties, structural modes, and discretization. The typical value is -18 dB per octave.

4) Estimate the frequency f_{st} and damping ξ of the lowest and dominant structural mode for each system configuration option.

5) Draw the high-frequency asymptote for each case such that each line passes through a corresponding point whose associated frequency and gain are f_{st} and $-(x + 20\log_{10}Q)$, where $Q = 1/\xi$.

6) Find the frequency f_c that corresponds to a point with the gain $-x$ on the preceding asymptote.

7) Draw the Bode step as a flat segment whose endpoint is f_c, its starting point is f_d, and its width is 1 octave. If the slope of the high-frequency rolloff corresponds to a third-order pole or less, 1 octave is usually sufficient; otherwise, the Bode-step width should be about 1.2 octaves.

8) Once f_c is determined in step 7, draw the low-frequency asymptotic line such that it passes through the starting point of the Bode step with a slope that was determined in step 2. Find the crossover frequency f_b where the line crosses the 0-dB level.

9) Assess the available control performance for each system configuration option.

10) Once choices are narrowed, approximate the associated Bode plots by rational transfer functions. Extract controller transfer function for each particular plant. Include nonlinear elements as required

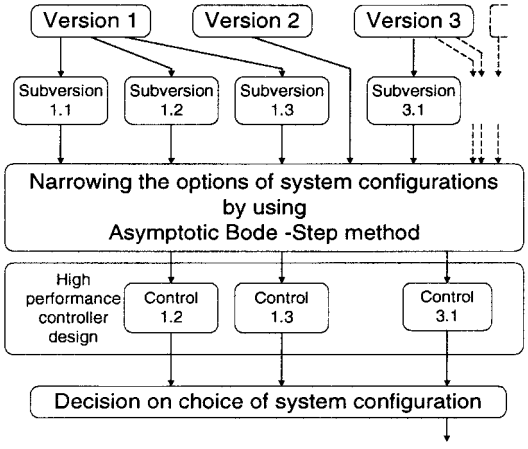

Fig. 8 Proposed evaluation of a concept design.

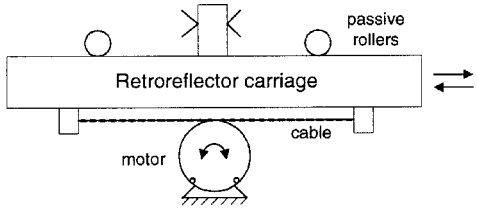

Fig. 9 Retroreflector carriage design.

in the compensator, and perform simulations to provide additional bases for tradeoffs. Figure 8 shows a diagram of the proposed evaluation of a concept design.

VI. Conceptual Design Example

The proposed Bode-step algorithm has been employed in the design process of the retroreflector carriage of a spacecraft interferometer subsystem shown in Fig. 9. The corner cube of the carriage is required to translate back and forth to vary the optical paths lengths of an optical interferometer.

The motion of the translator is cyclic and is expected to accelerate from rest, to settle to a constant rate of nearly 1 cm/s over 0.3 s, to maintain the rate for 4 s and sometimes for 16 s, and come to rest over 0.3 s. The motion then repeats. The performance of this subsystem is most stringent in rate and is required to follow the constant scan rate with a velocity ripple of no more than ±3%.

The carriage has several structural modes that are related to the longitudinal mode of the cable (about 100 Hz), bending mode of the rollers (about 116 Hz), and the rocking mode of the rollers (about 96 Hz). The average moment of inertia reflected to the motor axis is about 0.02 kgm^2. The motor drum radius is approximately 4 cm.

The preliminary control system design must assess performance for a set of mechanical plants with different structural modes and various friction characteristics. The data must be provided to system designers to choose appropriate encoder, motor, electronics, bearings type and preloads, and key elements in the supporting structure.

VII. Determination of the Available Feedback

Figure 10 shows a block diagram representation of the feedback control. The encoder data are sampled at 100 Hz and are used to calculate the input to the motor without substantial delays. Because the sampling frequency is close to the structural resonances, the resulting linear time-variable system has large phase shift uncertainty at the frequencies of the structural modes. Therefore, the modes must be gain stabilized.

As was stated earlier, the feedback bandwidth f_b is generally limited by sensor noise, sampling period, and plant structural modes. The encoder accuracy in this example is quite high. Therefore, the resulting quantization noise is not expected to impact the feedback bandwidth or shaping the loop gain.

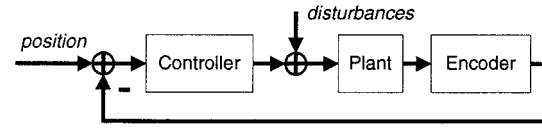

Fig. 10 Block diagram of the feedback loop.

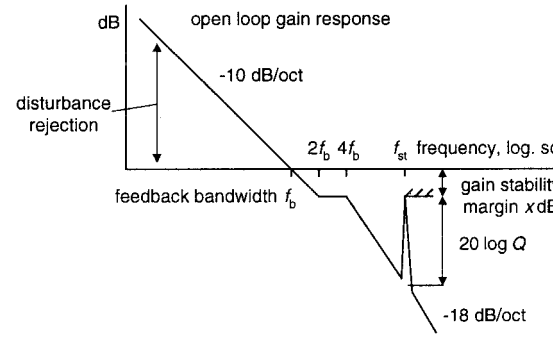

Fig. 11 Asymptotic Bode diagram.

The sampling frequency, however, limits the bandwidth. The conventional rule of thumb is to set the feedback bandwidth to be less than 10–15% of the sampling frequency, that is, less than 10–15 Hz.

The gain and phase stability margins are selected to be the typical values of 10 dB and 30 deg, respectively. As a result, the slope of the open-loop gain in the low-frequency range is about −10 dB per octave. The next step is to select the high-frequency rolloff. In this example, it is sufficient to characterize the high-frequency loop shape by a third-order pole, or equivalently, −18 dB per octave rolloff. This, together with the lowest frequency of the structural modes, implies that the feedback bandwidth f_b must satisfy the inequality

$$f_b < 0.25 f_{st} Q^{-\frac{1}{3}} = 0.25(96)(100)^{-\frac{1}{3}} \approx 5.2\,\text{Hz}$$

It then follows that the structural modes have the most impact on the feedback bandwidth. Therefore, the crossover frequency f_b is set to be 5.2 Hz. Figure 11 shows the resulting loop gain response.

As is seen, the described procedure easily shapes the loop based on minimal information on structural modes and target stability margins. The information from the given loop shape can be studied further to estimate the required frequency response of the prefilter, such that the total output-to-command response will be similar to that of a Bessel filter and time response characteristics such as rise time and settling time; this can be done without the actual design of the control laws.

The loop can easily be reshaped for different values of frequency and damping of structural modes. Figure 12 demonstrates the tradeoff results for different values of the frequency f_{st} and the quality factor Q. It is seen that, as f_{st} decreases or Q increases, the available feedback bandwidth and, consequently, the available disturbance rejection decrease. As a result, the rise time increases, which in turn degrades that available control performance.

As an example, suppose that the motor used in the servoloop has 45 slots. Then, the resulting motor reluctance cogging torque is a disturbance torque whose frequency is about 2 Hz for the specific scan rate of the servosystem. If the control bandwidth is 4 Hz, the cogging disturbance torque is amplified by positive feedback in the crossover area by about two times. However, for a control bandwidth of 10 Hz, this disturbance torque is attenuated by about two times. The difference in these two cases is about 12 dB. Such a difference is significant and serves as a motivating factor in the hardware selection process.

VIII. Controller Design

The application of the asymptotic Bode method is capable of reducing the number of available configuration options during the initial phase of a concept design. To finalize the particular choice of hardware, a more detailed analysis must be conducted that includes the effects of friction, uncertainties, sensor noise, unmodeled dynamics, phase delay, and discretization.

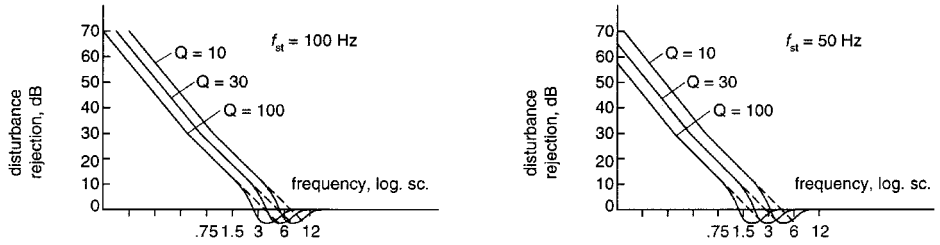

Fig. 12 Sensitivity results for different values of frequency and damping of the structural modes.

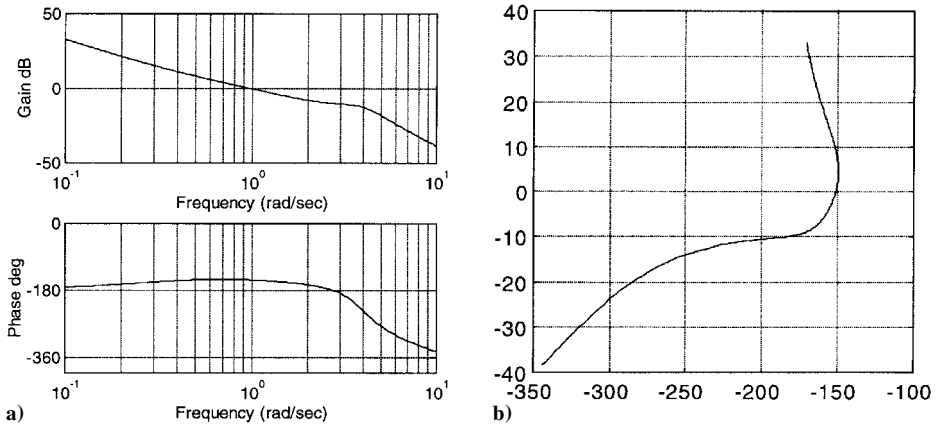

Fig. 13 Normalized open-loop response.

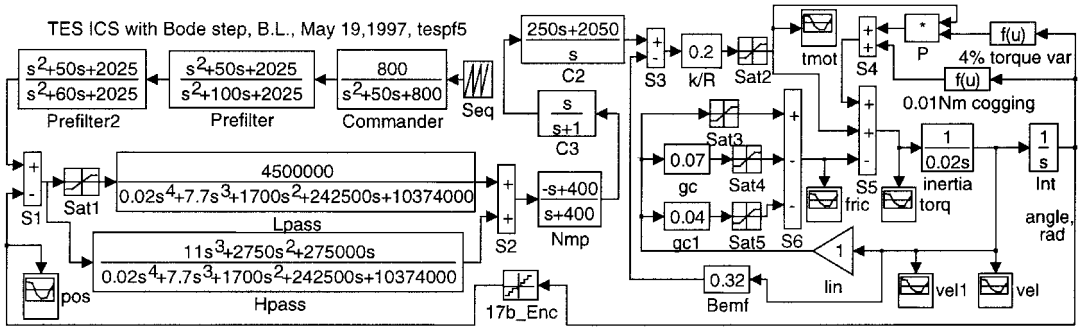

Fig. 14 Simulink block diagram.

The asymptotic Bode diagram developed in the preceding section can be approximated with rational transfer functions. Figure 13a shows the plot of the normalized transfer function

$$\frac{1}{s^2}\,\frac{11s^3+55s^2+110s+36}{s^4+7.7s^3+34s^2+97s+83}$$

with the crossover frequency of 1 rad/s, a Bode step of approximately 1 octave long, a low-frequency asymptotic slope of -10 dB per octave, a high-frequency asymptotic slope of -18 dB per octave, a gain margin of 10 dB, and a phase margin of 30 deg (Ref. 4). Figure 13b shows the associated Nyquist diagram in the L plane. It is then an easy task to extract a controller transfer function from the earlier loop design.

Suppose the normalized plant is represented by $1/s^2$. In addition, a nonminimum phase lag is also included in the plant model to account for the effect of sampling period. In this setting, the normalized plant transfer function is given by

$$P(s) = (1/s^2)[(10-s)/(10+s)]$$

and the corresponding normalized controller is

$$C(s) = \frac{11s^3+55s^2+110s+36}{s^4+7.7s^3+34s^2+97s+83}$$

Therefore, the normalized loop transfer function is

$$T(s) = C(s)(1/s^2)[(-s+10)/(10+s)]$$

The controller $C(s)$ can be decomposed further into the sum of low-pass and high-pass transfer functions and a saturation link installed in front of the low-pass path, as shown in Fig. 14, for the purpose of improving the system transient responses to large command.

The normalized prefilter function in the command path is

$$R(s) = \frac{s^2+\omega_b s+0.81\omega_b^2}{s^2+2\omega_b s+0.81\omega_b^2}\,\frac{s^2+0.5\omega_b s+\omega_b^2}{s^2+0.6\omega_b s+\omega_b^2}$$

The prefilter improves the linearity of the closed-loop system phase response and consists of two notches tuned at the frequencies close to the crossover.

The functions of the compensator and prefilter were denormalized for the crossover frequency to be 6 Hz, and the compensator was cascaded with a link

$$\frac{250s+2050}{s+1}$$

that together with the linearized plant produces the denormalized nominal plant.

IX. System Model and Simulation

The Simulink system model is shown in Fig. 14. The friction characteristic is static piece linear with certain stiction and coulomb level. The friction model includes saturation links and a summer. The slope of the friction torque can be adjusted with appropriate gain coefficients in the friction model. The coefficients have been chosen for the worst case: The stiction peak duration equals a half-period of the oscillation corresponding to the closed-loop controller.

With the use of Fig. 11, the feedback bandwidth (the crossover frequency) is chosen to be 6 Hz. The loop response is shaped with a Bode step, with 30-deg phase guard-point stability margin, with 10-dB gain guard-point stability margin, and with -18 dB/octave high-frequency asymptotic slope.

In the simulations, we use a motor model with torque constant 0.32 Nm/A and 1.7 Ω winding, with 4% torque variations as a function of the angle, with 45 slots, and with 0.01-Nm peak-to-peak ripples in the torque (of cogging). The plant equivalent moment of inertia relative to the shaft of the motor is 0.02 kgm^2.

The motor is driven by a voltage source, so that the relatively low motor winding resistance serves as the output impedance of the driver. As can be shown, in this case the motor cogging and torque variations have lesser effect on the controlled variables.

The compensator transfer function is split into low-frequency and high-frequency parallel paths. In front of the low-frequency path, a saturation link is placed with threshold 0.1 to improve the transient response to large amplitude commands and to provide global stability. The link $(-s+400)/(s+400)$ represents the phase delay associated with the sampling.

The simulation results are shown in Figs. 15–18. As seen in Fig. 15, the turn-around angle of 0.064 rad is covered in 0.3 s. As seen in Fig. 16, the angular velocity becomes constant as desired with better than 3% accuracy in approximately 0.15 s. On the velocity time history, the ripples at times up to 0.3 s are from the controller closed-loop response. The lower frequency ripples at larger times are from the cogging (the cogging will be smaller with an appropriate motor). The motor torque time history is shown in Fig. 17. The stiction and coulomb torque seen in Fig. 18.

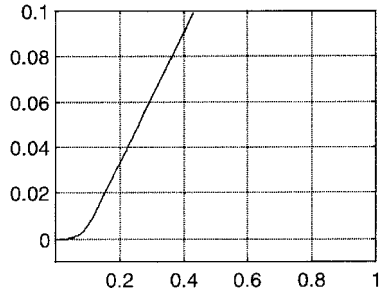

Fig. 15 Angle, radian.

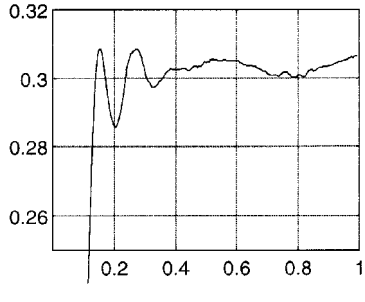

Fig. 16 Angular velocity, radian per second.

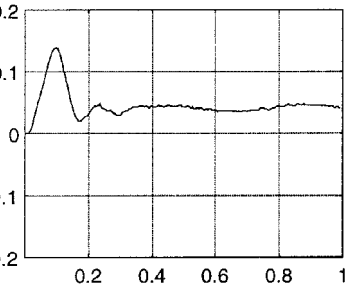

Fig. 17 Motor torque, newton meter.

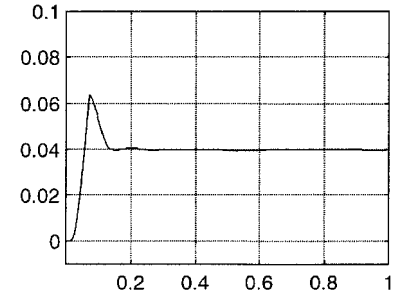

Fig. 18 Friction torque, newton meter.

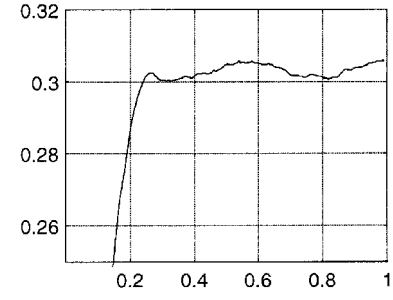

Fig. 19 Velocity plot when friction is absent.

Without friction, the velocity time history is shown in Fig. 19. The velocity settles to the required accuracy in 0.2 s. Bode-step toolbox MATLAB® functions facilitating the design are available for downloading, free for nonprofit use, from Lurie.[5]

X. Flexible Mode

From Fig. 3, it is seen that the chosen crossover frequency of 6 Hz corresponds to the flexible mode 100 Hz with $Q=15$. However, the modes in the plant are collocated, and due to the rather small ratio of the participating masses, the poles will be rather close to zeros, for example, within 20% in frequency. Then, the control system should be stable even with lower frequency of the flexible mode and with higher Q.

A collocated flexible mode with the frequency of the poles 60 Hz, of the zeros 50.3 Hz, and 0.01 damping was introduced in the plant as a cascaded link after the inertia link with transfer function

$$\frac{s^2+6.3s+100{,}000}{s^2+7.5s+142{,}000}$$

The flexible mode (the poles) are substantially damped by the low output impedance of the driver transformed into low output mobility of the motor (caused by the back emf loop in Fig. 14). However, when the driver is saturated, the damping effect decreases, and a system without substantial attenuation in the loop can be only conditionally stable and have a limit cycle. For this reason, substantial loop gain attenuation at the pole frequency provided by the Bode-step response is necessary.

The results of the obtained system simulation are very similar to those for the system without structural modes; the system remains stable.

XI. Conclusions

An asymptotic Bode-step technique based on Bode integrals was proposed for control systems' design during the design trades of complex aerospace systems. The method eliminates the need for designing control laws or designing a high-fidelity model to estimate the utmost available performance of a system during the initial design process. In addition, the method provides a simple tool for the extraction of a final controller design from a resulting optimal loop response in the final stages of a control system design.

The approach is to, first, find the theoretically best realizable transcendental loop responses under a set of easily accessible practical limitations, and, second, approximate the responses with high-order compensator functions. This approach is simple, straightforward,

and economical for both conceptual and the final design stages inasmuch as modern technology allows inexpensive and reliable implementation of high-order compensators[5] in the form of software or active analog circuitry. This results in substantial improvement of the system performance.

The benefits of using Bode integrals is demonstrated by several space application control systems' design in Ref. 4.

Acknowledgments

The research was carried out by the Jet Propulsion Laboratory, California Institute of Technology, under a Contract with NASA. The authors thank R. Laskin and E. Wong for discussions.

References

[1]Lurie, B., Laskin, R., and Wong, E., "Comparison of Using PID Preliminary Design and Simplified Bode Technique for the Purpose of Evaluating System Performance in Design Trade Studies," Jet Propulsion Lab., Engineering Memorandum 343-1165, California Inst. of Technology, Pasadena, CA, 1990.

[2]Bode, H. W., *Network Analysis and Feedback Amplifier Design*, Van Nostrand, New York, 1947, pp. 301, 321, 465–468.

[3]Lurie, B. J., *Feedback Maximization*, Artech House, Dedham, MA, 1986, pp. 61–75, 88–94.

[4]Lurie, B. J., and Enright, P. J., *Classical Feedback Control*, Marcel Dekker, New York, 2000, pp. 63, 64, 74–81, 97–105, 387.

[5]Lurie, B. J., "Discussions," URL: http://www.luriecontrol.com/Discussions.htm [cited 25 July 2000].